Monte Carlo dynamics study of motions in *cis*-unsaturated hydrocarbon chains

Y. K. Levine

Department of Molecular Biophysics, Buys Ballot Laboratory, University of Utrecht, 3508 TA Utrecht, The Netherlands

A. Kolinski

Department of Chemistry, University of Warsaw, Pasteura 1, 02-093 Warsaw, Poland

J. Skolnick

Department of Molecular Biology, Research Institute of the Scripps Clinic, La Jolla, California 92037

A Monte Carlo dynamics study of the motions of hydrocarbon chains containing *cis* double bonds is presented. The simulations utilize the high-coordination {2 1 0} lattice for the simultaneous representation of the tetrahedrally bonded carbon atoms and the planar unsaturated segment. Results on single chains undergoing free motion in space and tethered to an impenetrable planar interface are reported. The introduction of a *cis* double bond into a hydrocarbon chain induces a slowdown in the dynamics. The simulations show this to be a universal result independent of the representation of the chain on the lattice. In contrast, polyunsaturated chains are found to be more mobile than saturated ones.

I. INTRODUCTION

The characterization of the orientational and motional properties of hydrocarbon chains in lipid bilayer systems has been the subject of many experimental and theoretical investigations.[1-3] Despite these efforts, the full understanding of physical experiments in terms of the behavior of the hydrocarbon chains on a microscopic scale has been impeded by a variety of factors. These include the multiplicity of motions accessible to the lipid molecules and the implicit model dependence of the interpretation of the measurements. Consequently, questions pertaining to the nature of the motions, the importance of collective motions, and the extent and time scale of rotational diffusion have yet to be answered.

One of the most intriguing aspects of the work is the elucidation of the changes in the behavior of the alkane chains brought about by the introduction of *cis* double bonds. It is known that the position of the *cis* bond in a hydrocarbon chain influences the thermodynamic properties of the lipid bilayer.[2] For example, the transition temperature for a bilayer consisting of phosphatidylcholine molecules with chains 18 carbon long decreases by as much as 60 K as the unsaturated bond is moved away from the head group towards the 9–10 position in the middle of the chain.[4] The transition temperature, however, increases by the same amount for chains with a *cis* bond near the free terminal methyl group. Interestingly, naturally occurring lipids often possess a single *cis*-double bond in the chains at the 9–10 position (oleoyl chains).[1-3] The most common polyunsaturated 18 carbon chains contain unsaturated *cis* bonds in the lower half of the chain, in positions 9–10/12–13 (linoleoyl chains) or 9–10/12–13/15–16 (linolenoyl chains).[1-3] Increasing unsaturation in the lipid chains has been shown to cause a general decrease in the orientational order as monitored by ^2H nuclear magnetic resonance (NMR),[5] electron-spin resonance (ESR) spectroscopy,[6] and fluorescence depolarization.[7,8] However, the latter two techniques indicate that the reduction in order is accompanied by a slowdown in the rates of motion of the chains. This latter finding contrasts with the effect of increasing temperature which induces a reduction in the molecular order, but an increase in the rotational dynamics.

A greater insight into the dynamics of hydrocarbon chains and in particular, the effects of unsaturation on their motional properties, is only possible through the interpretation of the experimental data with theoretical simulations of chain motion. A number of molecular dynamics (MD) simulations have been performed previously on lipids containing alkane chains,[9-11] but these have been limited to time scales of 100 ps or less. Consequently, little has been learned concerning isomerizations, overall rotation, and the importance of collective motions in determining chain dynamics. In contrast, the technique of Brownian dynamics (BD)[12-16] covers the 10–100 ns time scale and lends itself to the study of local conformational motions. Indeed, the BD approach, rather than MD simulations, has proved useful in the analysis of ^{13}C relaxation time measurements in lipid systems.[16]

The time scale of the simulations of chain behavior can be extended even further by the use of Monte Carlo dynamics (MCD) techniques.[17,18] This method has been used with much success in the study of dynamic processes in polymer chains in melts and isotropic solvents.[17-19] It has also been applied recently to studies of the dynamics in monolayers of saturated lipid molecules.[20] The advantage of MCD over MD and BD simulations is that its fundamental time scale is that required for local conformational modifications. The efficiency of MCD is achieved by performing the simulations on a lattice which permits the use of fast integer arithmetic operations. An added advantage is the simplicity and rigor of the algorithms for avoiding bond cutting during the conformational changes. The technique is particularly attractive for studies of global relaxation phenomena, where the

detailed motions of the chains within local conformational wells become unimportant and in this respect complements MD and BD studies.

The drawback of the MCD technique, however, is the use of a lattice representation of the hydrocarbon chain. The diamond (tetrahedral) lattice is often used in the simulations as it reproduces the tetrahedral coordination of the carbon atoms (Fig. 1). Nevertheless, it has been found in practice that the computational advantages outweigh the simplifications arising from confining the chains to a lattice. Moreover, it has been shown for various polymer systems that this lattice representation works well and moreover, the simulations are in good agreement with the results of MD simulations in the intermediate to long time regime.[17-19]

While the diamond lattice provides a faithful representation of the rotational isomeric states of an alkane chain, it cannot reproduce the planar configuration of a *cis* double bond (Fig. 1). This is merely a reflection of the different coordinations of the sp^3 and sp^2 valence states of the carbon atoms.[1,2] In order to implement the MCD algorithms for unsaturated chains, we have utilized the high coordination {2 1 0} lattice.[21,22] This lattice has proved particularly successful in studies of the folding of polypeptide chains[21] and the range of dynamic moves it affords has been discussed in detail previously.[22]

Here we present an initial study of the dynamics of alkene chains using the {2 1 0} lattice representation. Results

on single chains undergoing free motion in space and tethered to an impenetrable planar interface are reported. We shall show that the introduction of a *cis* double bond into a hydrocarbon chain induces a slowdown in the chain dynamics, in qualitative agreement with experimental results on lipid bilayer systems.[6-8] Our findings indicate strongly that this is a universal result independent of the representation of the chain on the lattice. Interestingly, the simulations predict an enhancement of the rates of motion in the polyunsaturated linolenoyl chains.

The results of the simulations can be tested directly by carrying out NMR relaxation experiments on selectively labeled alkene and alkane chains. This work is in progress.[26] In addition, experiments on lipid bilayer systems containing linolenoyl chains are being undertaken using ESR and fluorescence depolarization techniques.

II. METHOD OF SIMULATION

A. Geometrical representation of chain molecules on a lattice

The model hydrocarbon chain consists of 18 beads connected by 17 bonds and is confined to a cubic lattice. On this lattice, the individual beads are separated by a distance of $\sqrt{5}$, and the bonds are obtained by a cyclic permutation of the 24 vectors of the type $\{\pm 2, \pm 1, 0\}$. One lattice unit is thus equivalent to a distance of 0.069 nm. The vectors are chosen from this basis set under the condition that the distance $R\,13$ between beads i and $i + 2$ lies in the interval $\sqrt{10} \leqslant R\,13 \leqslant \sqrt{18}$. Note that this does not faithfully reproduce the tetrahedral valence angle (109.47°) occurring in real alkane chains.[27] However, the choice was dictated by the need to obtain a uniform sampling of the allowed configuration space for isolated chains. We have found that simulations carried out with a fixed angle between pairs of adjacent vectors either led to kinetic trapping or to a biased sampling of the allowed chain configurations.

With this representation of the chain configuration, we have admitted the existence of multiple dihedral conformation states about each interior bond. It is important to note here that the conformational states occurred in pairs, characterized by a rotation of the same magnitude, but of opposite senses. This property is analogous to that of the *gauche* states of a real polymethylene chain[27] and ensures that on average the model chain is achiral.

The occurrence of multiple choices for the dihedral angles about the interior bonds leads to more disordered (coiled) conformations, with a resulting shorter end-to-end distance than would be expected for real alkane chains.[27] We have counteracted this artificial shortening of the chain by penalizing the probability of occurrence of the effective *gauche* states. The penalty was introduced by imposing restrictions on the distance $R\,14$ between the ith and $(i + 3)$th beads in the chain, thus effectively accounting for the so-called "pentane effect" in real chains.[27] This effect precludes the occurrence of the sequence *gauche* minus/*gauche* plus isomeric states about adjacent bonds as they lead to strongly repulsive steric interactions between nonbonded methylene groups. In our algorithms we rejected configurations in which $R\,14 \leqslant \sqrt{5}$ and accepted configurations with
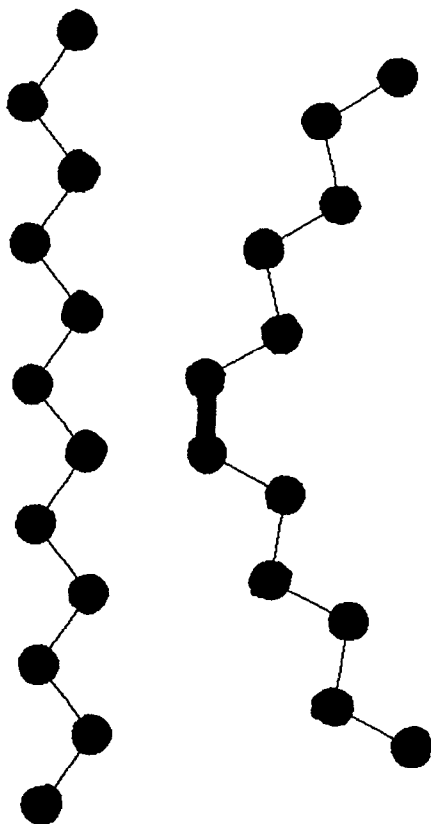

FIG. 1. A 12 atom alkane chain in the extended all-*trans* conformation (top) and a 12 atom alkene chain with a *cis* double at the central 6–7 position (bottom). The saturated segments of the alkene chain are in the all-*trans* conformation.

$\sqrt{5} < R\,14 \leqslant \sqrt{30}$ with a weighting factor of 20%. The value of the weighting factor was chosen such that it yielded end-to-end distances for the model saturated chain corresponding to those found for real alkane chains at ~350 K.[27]

In order to implement excluded volume effects, in particular to exclude chain cutting, every bead was surrounded by 12 occupied lattice sites, forming a face-centered-cubic (FCC) envelope about its position. These sites were obtained from the cyclic permutation of the vectors $\{ \pm 1, \pm 1, 0 \}$. This construction ensured that the chain was unable to cross itself on undergoing conformational changes.

The representation of the cis-double bond on our lattice was dictated by the planar configuration of the segment C–C = C–C.[1,2] Forty-eight distinct triplet vector combinations taken from the set $\{ \pm 2, \pm 1, 0 \}$ were found to produce a planar chain segment, though with valence angles differing from the expected value of 120°. We have found that in fact the geometrical representation of the unsaturated segments is of little consequence for the chain dynamics. The simulations show that the predominant effects on chain dynamics are due to the rigidity of this segment, i.e., the lack of rotations about the central C = C bond. We believe this to be a universal feature independent of the lattice representation of the chains.

B. Monte Carlo algorithm for chain motions

The time evolution of the model chain conformations was assumed to be described by stochastic kinetics. Thus, we employed a dynamic Monte Carlo technique to solve a stochastic kinetics master equation.[17,18] The use of this method to provide insight into the dynamics of macromolecular systems has a long history in polymer physics, where it has been shown to be in accord with the results of molecular dynamics simulations in the intermediate to long time regime.[17–19]

The conformational dynamics of the model saturated chain is assumed to arise from local rearrangements involving the transfer of a single bead, chosen at random, to a different lattice site, subject to the preservation of the length of the bonds to its two neighboring atoms. In this way, new conformations can be introduced locally.

The first (or last) bond is allowed to undertake random orientations. These latter moves introduce new local orientations which diffuse into the interior parts of the chain. This set of local modifications is found to span all possible conformations of the chain and allows the study of its dynamic properties.

The rigidity of the segment containing a cis double bond necessitated the introduction of larger scale moves involving two or three beads. A four-bond motion was required if the first (or last) bead of the –C–C = C–C– segment (Fig. 1) is picked. This move involves the double bond itself and either the two preceding or two following bonds. Three beads are thus involved in a move which keeps all the other beads of the chain in fixed positions. A three-bond move is allowed if either of the two beads connected by the double bond are picked. This move involves a simple interchange of the two adjacent single bonds, thus conserving the configuration of the unsaturated segment.

In addition, the penalty imposed on the distances $R\,14$ was modified in the neighborhood of the cis double bond. This is necessary in order to account for the important fact that there is little steric hindrance to rotation about the single bonds immediately adjacent to the cis bond.[23,24,27] This was implemented simply by allowing all values for the distance $R\,14$ which includes the cis double bond. Effectively, this means that the cis double bond decouples the effects of steric hindrance between the two chain segments joined to it.

The chosen moves are subjected to two acceptance tests. In the first place, the new $R\,14$ distances between the beads involved in the move and their neighbors are checked and the move allowed only if it satisfies the criteria set out above. Second, the move is only accepted if the final lattice positions of the beads are unoccupied. This test is applied to both a bead and its associated FCC envelope.

The fundamental time step of the algorithm is taken to be such that every bead in the chain has an equal chance of undergoing a motion.[17,18] This is achieved simply by attempting 18 moves, with each bead having an equal probability of being picked. It must be emphasized that this time step is not defined on an absolute scale.

The correlation functions for motion are obtained on invoking the ergodic hypothesis and replacing ensemble averages over a calculated trajectory in configuration space by time averages. The decay of the time correlation function $G(t)$ of the end-to-end vector $\mathbf{R}(t)$, $G(t) = \langle \mathbf{R}(0) \cdot \mathbf{R}(t) \rangle$ was used to determine the length of the computed trajectory. The total time of the simulation was chosen such that this function decayed to less than 10% of its initial value.

We have typically computed 2×10^5 configurations at intervals of 40 elementary time steps for the saturated chains and 100 time steps for chains containing cis double bond segments. The correlation functions were computed out to times corresponding to not more than 1000 intervals. With this choice, the statistical fluctuations in the calculated average chain parameters obtained from runs starting with different initial conformations varied by less than 10%. The time correlation functions exhibited deviations between runs mostly after decaying to less than 30% of their initial values. The calculation of a trajectory for the saturated chain required about 90 minutes central processing unit (CPU) time (about 4 h for an unsaturated one) on a Sparc 1 + workstation.

III. RESULTS AND DISCUSSION
A. Free chain
1. Saturated chains

The chain configurations obtained from a simulation run consisted on average of the following $R\,13$ distances: 4% with $R\,13$ equal to $\sqrt{10}$ and $\sqrt{12}$, 25% with $R\,13 = \sqrt{14}$, 11% with $R\,13 = \sqrt{16}$, and 56% with $R\,13 = \sqrt{18}$. The distribution of the square end-to-end distance R^2 of the saturated chains was found to be fairly narrow with a standard deviation of 10% around the average value of $\langle R^2 \rangle \approx 500$. This was also reflected in the decay of time correlation function of the end-to-end vector which was found to be domi-

nated by orientational changes. The probability of a *trans* conformation about any bond in the chain was found to be 0.195–0.200, except for the two terminal bonds where a somewhat lower probability 0.18 was observed. These findings are consistent with the results of the rotational isomeric state theory for polymethylene chains.[27]

Every bond vector in the chain was found to be essentially uniformly distributed over the 24 basis vectors. The small deviations from the uniform distribution were statistical in character and varied from run to run.

In order to gain insight into the dynamics of the chain, we divided the chain into four equal segments and considered the vectors connecting beads four bonds apart: 1–5, 5–9, 10–14, and 14–18. This division is symmetric about the center of symmetry of the chain at the bond connecting beads 9 and 10. We thus expect the vectors R 1–5 and R 14–18 as well as R 5–9 and R 10–14 to exhibit the same dynamic behavior. This in fact forms a stringent test of the simulations. In addition, we also considered the vector R 7–12 which appears to reflect closely the average behavior of the chain. This coarse sampling of the chain behavior was chosen as we expect it to be less sensitive to the details of motion conferred by the underlying lattice.

The time correlation function $G_1(t) = \langle \cos\beta(0) \cdot \cos\beta(t)\rangle$ was calculated for each of the five chain segments under consideration. Here β is the angle between the given vector and an arbitrary fixed vector in the lattice. The decay of the correlation function was found to be virtually independent of the choice of reference vector, the deviations being of the same order as the statistical fluctuations observed between the results of different runs. This indicated that the orientational motions of the chain segments were isotropic. Consequently, we chose the Z axis of the lattice as our reference direction for ease of computations.

The temporal behavior of the correlation functions for the motion of the vectors R 1–5, R 5–9, and R 7–12 are shown in Fig. 2 for a saturated chain. The value of the correlation function at time $t = 0$ was found to be 0.33 ± 0.01, close to the value of 0.333 expected for a uniform sampling of the angles β. We have therefore normalized the correlation functions relative to time $t = 0$. The rates of motions are characterized by the generalized correlation time τ, defined as the area under the normalized correlation function. The correlation time was obtained numerically from a least-squares fit of $G_1(t)$ to a triexponential decay function.

The decay of $G_1(t)$ for the R 10–14 and R 14–18 vectors is indistinguishable from that shown in Fig. 2 for the R 5–9 and R 1–5 vectors, respectively, and the corresponding correlation times are given in Table I. The decay of the outer segmental vectors R 1–5 and R 14–18 is significantly faster than that for the inner vectors R 5–9 and R 10–14. However, the correlation function for the vector R 7–12 which spans the center of mass of the chain, decays more slowly than those for the other vectors. This correlation function is more sensitive to the reorientational modes of the chain as a whole; its decay is affected to a lesser degree by the internal modes of motion.

It turns out that the rate of decay of the correlation functions is sensitive to the effects of steric hindrance, or in
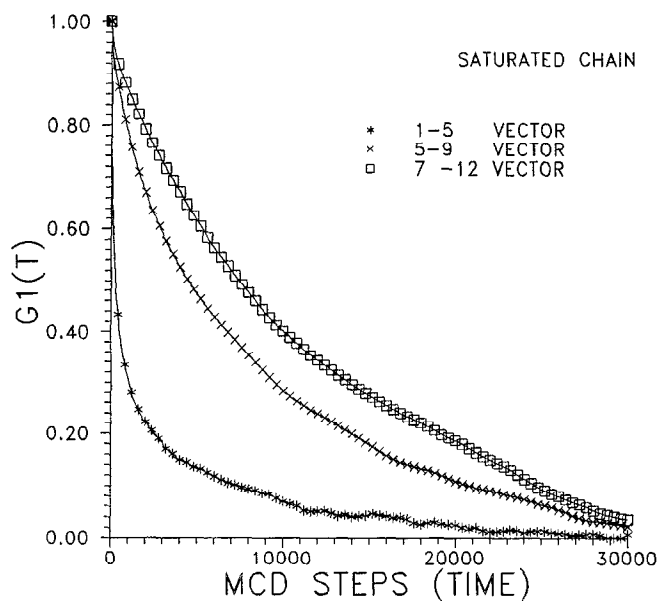

FIG. 2. The time-correlation functions $G_1(t)$ (see the text) for the vectors in a saturated 18 bead model alkane chain with free terminal motion. The correlation functions for the pairs of vectors (R 1–5, R 14–18) and (R 5–9 and R 10–14) are virtually indistinguishable and reflect the symmetry of the chain about the 9–10 bond.

our case, the restrictions imposed on the R 14 distances in the chain. A much faster decay of $G_1(t)$ is observed for the athermal model chain, i.e., in the absence of any restrictions on R 14. Now the differences in the decays of the inner and outer vectors is considerably smaller. The observed differences are due solely to the diffusion of new orientations from the terminal bonds into the center of the chain. Nevertheless, $G_1(t)$ for the vector R 7–12 exhibits an appreciably slower decay reflecting the overall orientational motion of the chain.

The effects of steric hindrance on the dynamics of the model chain can be rationalized as follows. The restrictions on the distances R 14 introduce a cooperativity into the conformational motions by precluding certain conformational sequences about neighboring bonds. The consequences of cooperativity on the chain dynamics are marked for the motions of the central segments of the chain as they are coupled to the outer segments. However, the terminal segments which are bonded only at one end can undergo rapid and unrestricted end relaxation.

TABLE I. The generalized correlation times characterizing the rates of motion of free chains. The values are given in units of MCD time steps.

	R 1–5	R 5–9	R 10–14	R 14–18	R 7–12
Chain					
Saturated	2 600	8 450	8 550	2550	11 000
3–4 *cis*	4 125	18 100	15 300	3800	21 800
6–7 *cis*	14 600	92 500	15 400	4260	51 800
9–10 *cis*	1 350	54 000	54 500	1300	160 000
9–10/12–13 *cis*	1 350	17 500	160 250	9200	122 000
9–10/12–13/15–16 *cis*	1 425	2 900	2 100	825	2 475

2. Chains containing cis segments

Simulations of chains with the *cis* double bond at the 3–4, 6–7, 9–10, 12–13, and 15–16 chains were carried out using the motions of the beads described above. Identical results were obtained for the 3–4 and 15–16 chains as well as for the 6–7 and 12–13 ones reflecting the symmetry properties of the 18 bead chains. Consequently, we shall here consider only the three chains 3–4, 6–7, and 9–10 which exhibit distinct properties.

The distributions of the square end-to-end distance R^2 of the chains were found to be as narrow as those shown by the saturated chains. However, the center of the distribution $\langle R^2 \rangle \approx 450$ for the 3–4 unsaturated chain and $\langle R^2 \rangle \approx 405$ for the 6–7 and 9–10 chains was significantly lower than found for the saturated chains $\langle R^2 \rangle \approx 500$. The probability of a *trans* conformation about any bond in the center of the chain was found to be 0.195–0.200, except for the two bonds adjacent to the *cis* double bond. Here a lower probability of 0.12–0.13 was found, somewhat higher than the value of 0.094 expected in our model for a chain with no steric hindrance for bond rotations. The *cis* double bond vector in every chain was found to be essentially uniformly distributed over the 24 possible basis vectors. The small deviations from the uniform distribution were statistical in character and varied from run to run.

The correlation functions $G_1(t)$ for the end-to-end vectors exhibited substantially slower decays than that obtained from simulations of the saturated chain. Moreover, the decay slowed down markedly on moving the *cis* double bond from the 3–4 position to the center of the chain at the 9–10 position. Again, the decay was predominantly due to the orientational motions of the end-to-end vector. This slowdown necessitated the computation of much longer trajectories than was the case for the saturated ones. Our choice of an increase in the simulation time by a factor of 2.5 represents a useful compromise between the length of the run and statistical significance.

The slowdown in the dynamics of the orientational modes of motion was also reflected in the correlation functions of the chain segments containing the *cis* double bond. At the time origin, the correlation functions for the four chain vectors were found to have a constant value $G_1(0) = 0.33 \pm 0.01$ as expected for a random orientational distribution in space. We have therefore normalized the correlation functions so that $G_1(0) = 1$. The correlation functions were computed relative to the Z axis of the lattice for convenience as the same behavior was obtained if an arbitrary lattice vector was chosen.

Figures 3–5 show the orientational correlation functions $G_1(t)$ for the motions of the vectors R 1–5, R 5–9, R 10–14, R 14–18, and R 7–12 for the chains with the *cis* bonds at the 3–4, 6–7, and 9–10 positions. The corresponding correlation times are given in Table I.

Interestingly, the decays found for the symmetric chain containing the *cis* double bond at the 9–10 position exhibit not only the expected symmetry, but are also faster than those observed for the saturated chain. Only the vector R 7–12 exhibits the slowdown in the orientational dynamics. All the correlation functions were found to exhibit long time
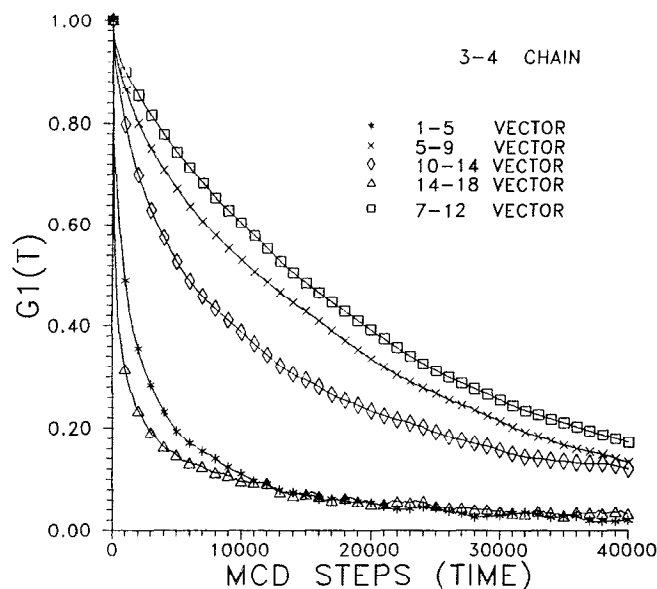

FIG. 3. The time-correlation functions $G_1(t)$ (see the text) for the vectors of an 18 bead model alkene chain with a *cis* double bond at the 3–4 position. Both terminal ends of the chain undergo unrestricted motion.

tails accounting for up to 30% of the amplitude at $t = 0$. This contribution depends strongly on the relative position of the vector and the *cis* double bond.

The question now arises as to whether the slowdown in dynamics caused by the introduction of a *cis* double bond is a real physical effect or an artifact of the rules for bond motions underlying the model. In this context, we need to note that a short chain containing six beads with a *cis* bond at the 3–4 (symmetry) position exhibits a correlation function for the 1–6 vector virtually indistinguishible for that computed
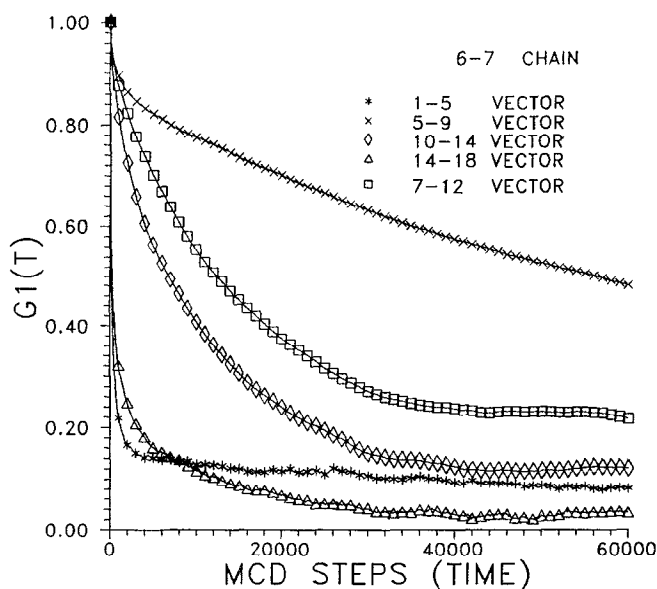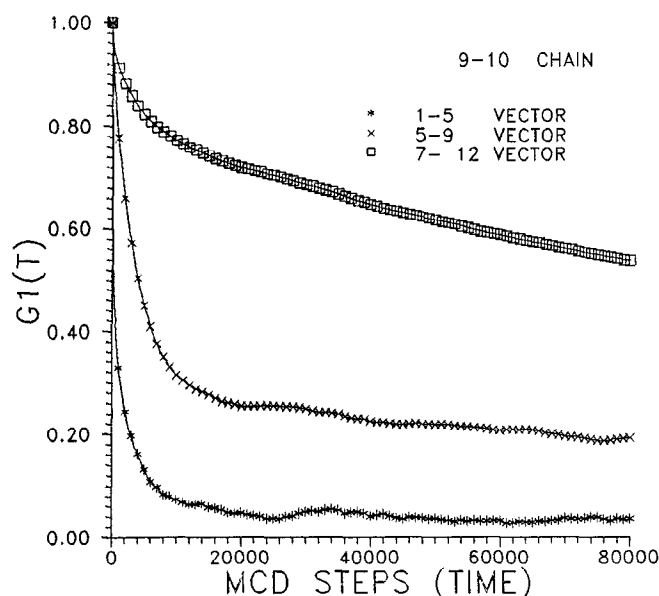

FIG. 4. The time-correlation functions $G_1(t)$ (see the text) for the vectors of an 18 bead model alkene chain with a *cis* double bond at the 6–7 position. Both terminal ends of the chain undergo unrestricted motion.

FIG. 5. The time-correlation functions $G_1(t)$ (see the text) for the vectors of an 18 bead model alkene chain with a *cis* double bond at the 9–10 position. Both terminal ends of the chain undergo unrestricted motion. The functions for the pairs of vectors (R 1–5, R 14–18) and (R 5–9 and R 10–14) are virtually indistinguishible and reflect the symmetry of the chain about the 9–10 bond.

for a six-bead saturated chain. This, taken with the observation of an isotropic distribution of orientations of the double bond vector in space, indicates that the intrinsic motions assigned to the rigid *cis* segments do not by themselves account for the slowdown in dynamics. The dynamic effects arise simply from the restrictions on the motions of the rigid *cis* double bond segment due to its attachment on both sides to fairly immobile chain segments. This can indeed be seen from Figs. 3–5, which show that the slow-down effects become progressively more significant as the *cis* double bond is moved away from the free terminal towards the middle of the chain. It appears that the rigid segment forms a bottleneck for the diffusion of new orientations along the chain. We note further that the rigid *cis* double bond segment also decouples the cooperative motions within the chain due to steric hindrance, so that the saturated segments become somewhat more mobile in the unsaturated chain than in a saturated one of the same overall length.

Our conclusions that the insertion of a rigid structural entity into an otherwise flexible chain introduces a bottleneck for the diffusion of new orientations along the chain are reinforced by simulations of chains containing a nonplanar conformation for the *cis* double bond. There are 48 distinct vector triplets representing each optical isomer of the segment. The slowdown in the dynamics is again observed if the *cis* segment is restricted to the configuration of a single isomer. However, the dynamics revert to those observed for a saturated chain on allowing interconversions between the two isomers during the conformational motions. This is equivalent to admitting hindered rotations about the double bond.

Further evidence supporting our contentions is provided by simulations of polyunsaturated chains containing

cis double bonds in the 9–10/12–13 and 9–10/12–13/15–16 positions. The correlation functions $G_1(t)$ for these chains are shown in Figs. 6 and 7. The chain containing two *cis* double bonds exhibits the slowdown in dynamics, particularly for the vectors near the *cis* double bonds (Table I). However, the chains containing three *cis* double bonds exhibit rapid decays, faster even than those found in the saturated chains (Table I). We note that these chains consist of a wholly unsaturated segment attached to a saturated one. Only the short, seven bead long, saturated segment is subject to steric hindrance effects. Consequently, this segment exhibits faster motions than a corresponding segment in an 18 bead chain. The mismatch between the motions of the two segments is now only operative at the point of their attachment in the middle of the chain. Work is currently under way using Brownian dynamics to examine the lattice independence of the results.[25]

B. Tethered chains

The chains were constrained to move freely over a plane, e.g., the XY plane of the lattice, but the first bead was only permitted to move by one lattice unit along the normal to the plane, the Z axis. Furthermore, the chain was restricted to the half-space above the plane, so that it occupied lattice sites whose Z coordinate was positive. This was implemented simply in the algorithm by a permanent occupation of the lattice sites in the negative half-space. The XY plane was chosen for convenience, as identical results were obtained from simulation runs using other crystallographic planes of the cubic lattice.

It is important to note that now the orientational average $\langle \cos \beta \rangle$, the order parameter $\langle P_1 \rangle$, does not vanish identically if the vector orientations are restricted to the interval
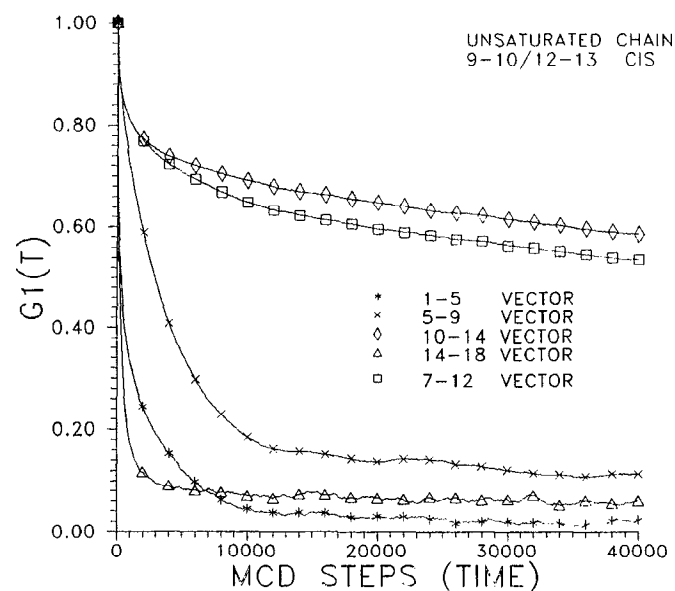

FIG. 6. The time-correlation functions $G_1(t)$ (see the text) for the vectors of an 18 bead model alkene chain with two *cis* double bonds at the 9–10 and 12–13 positions. Both terminal ends of the chain undergo unrestricted motion.
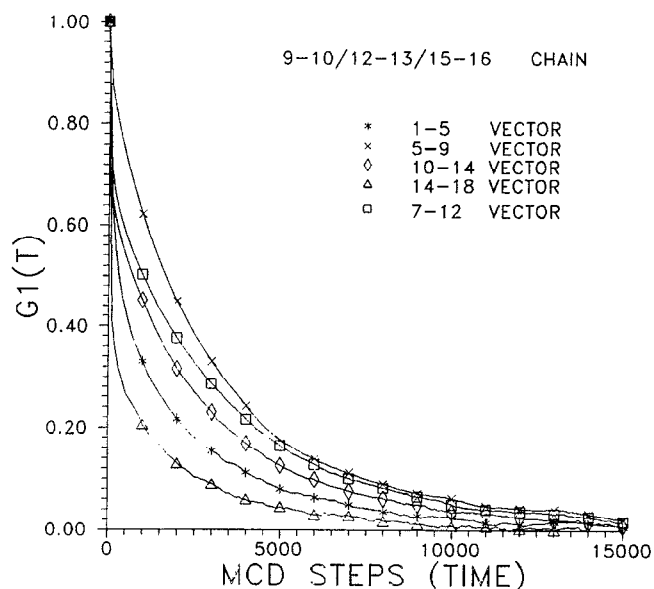
FIG. 7. The time-correlation functions $G_1(t)$ (see the text) for the vectors of an 18 bead model alkene chain with three *cis* double bonds at the 9–10, 12–13, and 15–16 positions. Both terminal ends of the chain undergo unrestricted motion.

$0 \leqslant \cos \beta \leqslant 1$. Consequently, the correlation function $G_1(t)$ will decay to a constant plateau at long times, such that $G_1(t \to \infty) = \langle \cos \beta \rangle^2$. At time $t = 0$, we have $G_1(0) = \langle \cos^2 \beta \rangle$. For a uniform distribution of orientations over the half-plane, we expect $\langle \cos \beta \rangle = \frac{1}{2}$ and $\langle \cos^2 \beta \rangle = \frac{1}{3}$.

In this case, we define the correlation time τ as

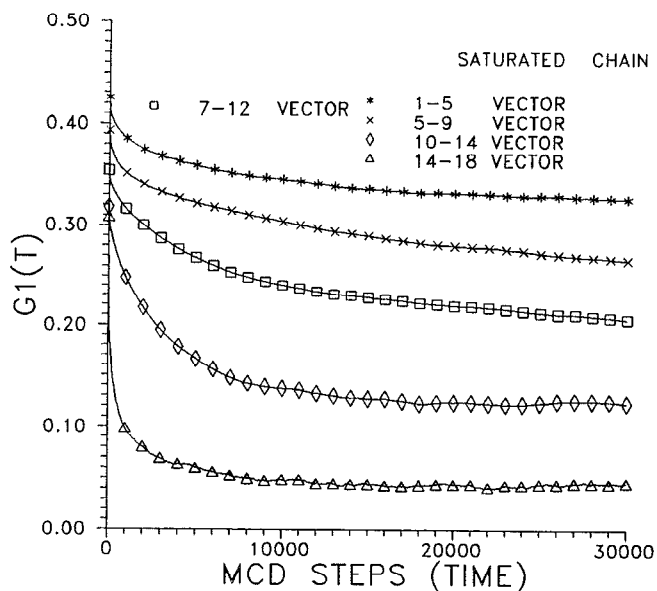$$\tau = \int_0^\infty [G_1(t) - G_1(\infty)] dt / [G_1(0) - G_1(\infty)] \tag{1}$$

FIG. 8. The time-correlation functions $G_1(t)$ (see the text) for the vectors in a saturated 18 bead model alkane chain tethered to the impenetrable XY plane. The first bead is allowed to move up and down the Z axis by one lattice unit.

again corresponding to the area under the normalized correlation function. For computational purposes, we have truncated the integral after 40 000 MCD time steps as to a good approximation $G_1(40\,000) \sim \langle \cos \beta \rangle^2$.

1. Saturated chains

Figure 8 shows the decay of $G_1(t)$ for a saturated chain composed of 18 beads. The decrease in the values of $G_1(0)$ as well as of the heights of the long time plateaus indicates that the motions of the vectors become less restricted on moving from the tethered first bead towards the free terminal of the chain. Indeed, these values indicate that the vectors R 10–14 and R 14–18 can access an almost uniform distribution of orientations ($-1 \leqslant \cos \beta \leqslant 1$) relative to the Z axis, the normal to the plane. However, the orientations of the first two vectors R 1–5 and R 5–9 are restricted by the presence of the impenetrable XY plane to the range $0 \leqslant \cos \beta \leqslant 1$. The R 7–12 vector exhibits an intermediate behavior which may be identified with the average motion of the chain.

The effective correlation times for the motions of the four vectors R 1–5, R 5–9, R 10–14, and R 14–18 are given in Table II. The progressive decrease of τ on moving from the tethered head to the free terminal segment of the chain is consistent with the observed increased range of orientations of the vectors. Interestingly, a smaller value of τ is found for the initial 1–5 segment than for the 5–9 segment. Again the motion of the R 7–12 vector reflects the average chain motion.

2. Cis-unsaturated chains

The tethering of the chains to the plane has effectively removed the center of symmetry of the chain, so that now a distinct behavior is expected for chains containing *cis* double bonds at different places along the chain. This is illustrated in Fig. 9, where the correlation functions $G_1(t)$ for the 9–10 chain are shown. A comparison of Figs. 8 and 9 shows that the motions of R 5–9 and R 7–12 are more restricted in the unsaturated chain than in the saturated one. In marked contrast, the introduction of the *cis* double bond allows the vectors R 10–14 and R 14–18 to access a larger range of orientations. This is consistent with our conclusions above about the influence of the steric hindrance factor on chain motion.

The effective correlation times (Table II) yield a different picture of chain dynamics. The values for all these parameters, with the exception of that for R 5–9, are found to be significantly higher than those of the saturated chain.

TABLE II. The generalized correlation times characterizing the rates of motions of tethered chains. The values are given in units of MCD time steps.

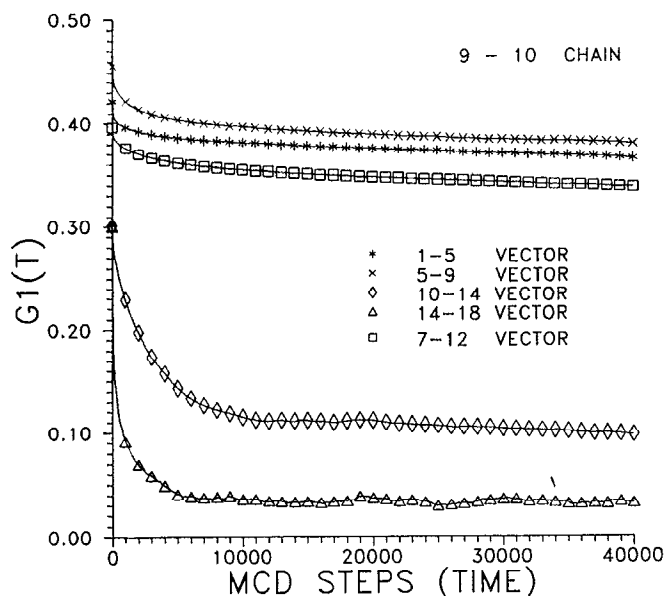| Chain	R 1–5	R 5–9	R 9–10	R 14–18	R 7–12
Saturated	5 550	7 600	3 260	800	6 900
3–4 *cis*	13 000	10 800	6 000	1400	10 500
6–7 *cis*	10 100	9 700	6 130	1500	7 100
9–10 *cis*	8 600	6 680	4 350	1030	8 850
12–13 *cis*	6 000	7 600	12 000	1600	8 600
15–16 *cis*	6 200	8 000	8 050	3500	9 200
9–10/12–13 *cis*	7 650	6 050	7 400	1000	6 450
9–10/12–13/15–16 *cis*	7 620	4 000	2 400	780	1 240

FIG. 9. The time-correlation functions $G_1(t)$ (see the text) for the vectors in an 18 bead model alkene chain containing a *cis* double bond at the 9–10 position. The chain is tethered to the impenetrable XY plane, but the first bead is allowed to move up and down the Z axis by one lattice unit.

FIG. 11. The time-correlation functions $G_1(t)$ (see the text) for the vectors in an 18 bead model alkene chain containing three *cis* double bonds at the 9–10, 12–13, and 15–16 positions. The chain is tethered to the impenetrable XY plane, but the first bead is allowed to move up and down the Z axis by one lattice unit.

Simulations of chains containing *cis* double bonds at the 3–4, 6–7, 12–13, and 15–16 positions show that in general the introduction of the double bond tends to lower the orientational averages of the vectors. The most significant effects being observed are for the 6–7 chain.

However, the most striking feature of the correlation functions is the substantial increase of the effective correlation times relative to those of the saturated chain (Table II).
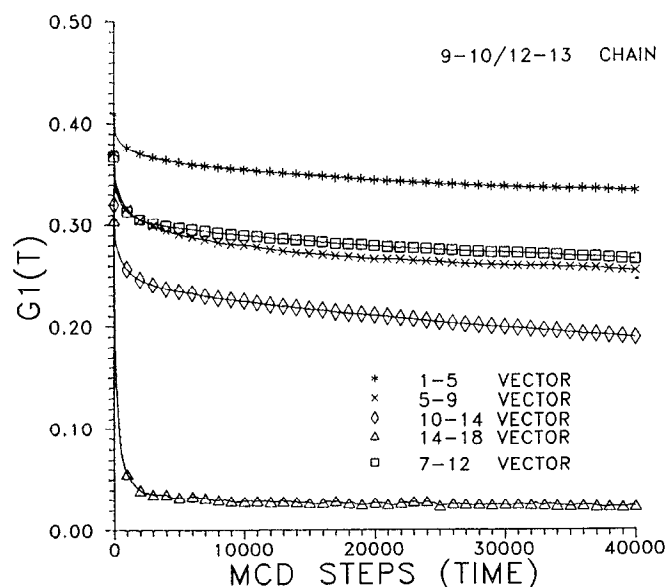

FIG. 10. The time-correlation functions $G_1(t)$ (see the text) for the vectors in an 18 bead model alkene chain containing two *cis* double bonds at the 9–10 and 12–13 positions. The chain is tethered to the impenetrable XY plane, but the first bead is allowed to move up and down the Z axis by one lattice unit.
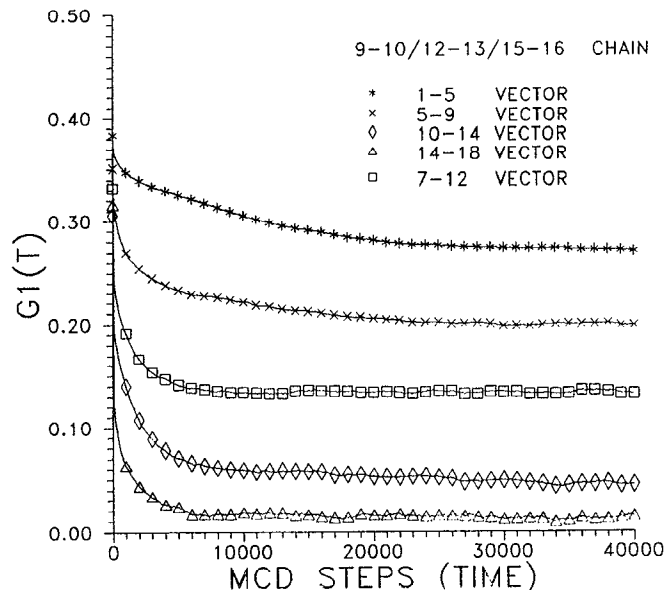
The largest effects are found for the segments adjacent to or containing the *cis* double bond. The only exceptions are the R 1–5 and R 5–9 vectors in the 12–13 and 15–16 chains which exhibit similar correlation times to those of the saturated chains.

The most remarkable effects of unsaturation on the dynamics of the chains are observed in polyunsaturated chains. The correlation functions $G_1(t)$ for chains containing *cis* double bonds at the 9–10/12–13 and 9–10/12–13/15–16 positions are shown in Figs. 10 and 11, respectively. The introduction of a second double bond at the 12–13 position can be seen to cause a significant reduction in the orientational parameters of the R 10–14, R 14–18, and R 7–12 vectors. The third *cis* double bond at the 15–16 position further reduces these parameters. Thus the motions of the vectors in these chains are less restricted than those in the equivalent saturated case.

The correlation times for the 9–10/12–13 chain (see Table II) are similar to those observed for the 9–10 chain with two clear exceptions. A large increase is found for the R 10–14 vector (from 4400 to 7400 time steps), but a large decrease (from 8900 to 6400 time steps) for the correlation time of R 7–12. The additional bond at position 15–16, however, causes a marked reduction in all the correlation times beyond R 1–5 (Table II). These are in fact significantly lower than those found for the saturated chain with the sole exception of that for the initial segment. We note that a similar effect was described above for the free chain.

These results indicate that there is no simple relation between the restriction on the angular excursions of the vectors as reflected by the orientational averages and the correlation times defining the rates of reorientational motions. This finding is in agreement with experimental observations of the behavior of lipid bilayer systems.[6-8]

ACKNOWLEDGMENTS

[1] D. M. Small, in *The Physical Chemistry of Lipids*, edited by D. J. Hanahan (Plenum, New York, 1986), Vol. 4.

[2] B. L. Silver, *The Physical Chemistry of Membrane* (Solomon, New York, 1985).

[3] M. D. Houslay and K. K. Stanley, *Dynamics of Biological Membranes* (Wiley, Chichester, 1982).

[4] P. G. Barton and F. D. Gunstone, J. Biol. Chem. **250**, 4470 (1975).

[5] A. Seelig and J. Seelig, Biochemistry **16**, 45 (1977).

[6] L. J. Korstanje, E. E. van Faassen, and Y. K. Levine, Biochim. Biophys. Acta **982**, 196 (1989).

[7] G. Deinum, H. van Langen, G. van Ginkel, and Y. K. Levine, Biochemistry **27**, 852 (1988).

[8] G. van Ginkel, H. van Langen, and Y. K. Levine, Biochimie **71**, 23 (1989).

[9] P. van der Ploeg and H. J. C. Berendsen, J. Chem. Phys. **76**, 3217 (1982); Mol. Phys. **49**, 233 (1983).

[10] S. Northrup, J. Phys. Chem. **88**, 3441 (1983).

[11] A. J. Kox, J. P. J. Michels, and F. W. Wiegel, Nature **287**, 317 (1980).

[12] E. Helfland, Z. R. Wasserman, and T. A. Weber, Macromolecules **13**, 526 (1980); J. Skolnick and E. Helfland, J. Chem. Phys. **72**, 5489 (1980).

[13] R. M. Levy, P. G. Woylnes, and M. Karplus, J. Am. Chem. Soc. **103**, 5998 (1981).

[14] C. James and G. T. Evans, J. Chem. Phys. **76**, 2680 (1982).

[15] W. F. van Gunsteren, H. J. C. Berendsen, and J. A. C. Rullmann, Mol. Phys. **44**, 69 (1981).

[16] R. W. Pastor, R. M. Venables, and M. Karplus, J. Chem. Phys. **89**, 1112 (1988).

[17] *Monte Carlo Methods in Statistical Physics*, edited by K. Binder, (Springer, Berlin, 1986).

[18] J. Skolnick and A. Kolinski, Adv. Chem. Phys. **78**, 223 (1990).

[19] A. Baumgartner, Annu. Rev. Phys. Chem. **35**, 419 (1984).

[20] M. Milik, A. Kolinski, and J. Skolnick, J. Chem. Phys. **93**, 4440 (1990).

[21] J. Skolnick and A. Kolinski, Science **250**, 1121 (1990).

[22] A. Kolinski, M. Milik, and J. Skolnick, J. Chem. Phys. **94**, 3978 (1991).

[23] J. Skolnick and E. Helfland, J. Chem. Phys. **72**, 5489 (1980).

[24] J. Skolnick, Macromolecules **14**, 646 (1981).

[25] A. Rey and J. Skonick (unpublished).

[26] R. R. Vold (personal communication).

[27] P. J. Flory, *Statistical Mechanics of Chain Molecules* (Interscience, New York, 1969).